Personalizing the Pressure Reactivity Index for Neurocritical Care Decision Support

Jennifer K. Briggs, J.N. Stroh, Brandon Foreman, Soojin Park, the TRACK-TBI Study Investigators, Tellen D. Bennett, David J. Albers

***Abstract*— Neurocritical care patients may benefit from personalized care based on their cerebral autoregulatory function. The pressure reactivity index is an important, prevalent metric used to estimate the state of a patient's cerebral autoregulation and guide clinical decision-making. The pressure reactivity index is calculated by first averaging arterial blood pressure and intracranial pressure signals over a time window and then correlating multiple of these averaged samples. In this manuscript, we use simulated and traumatic brain patient data to evaluate the effect of the size of averaging and correlation windows on the pressure reactivity index estimation. We show that the pressure reactivity index is sensitive to averaging and correlation windows, and the type of sensitivity is heterogeneous across patients. After a comprehensive analysis, we recommend an optimal averaging window of 9-10 seconds and a correlation window from 40-55 samples. Due to the heterogeneous sensitivity across patients, we also suggest that the pressure reactivity index can be made patient-specific by averaging over heartbeats rather than seconds. Implementing this novel heartbeat pressure reactivity index methodology decreases bias, uncertainty, and sensitivity in the pressure reactivity index. Clinical decision-making based on the pressure reactivity index may be a helpful step in personalizing medicine in neurocritical care patients and improving patient outcomes. Here, we suggest two ways to improve the robustness of the pressure reactivity index, allowing it to be more clinically useful and applicable to other populations, such as pediatrics.**

J.K.B and D.J.A are with Department of Bioengineering, University of Colorado Anschutz Medical Campus, Aurora CO (email: Jennifer.Briggs@cuanschutz.edu)

J.K.B, J.N.S, T.D.B, and D.J.A are with Department of Biomedical Informatics, University of Colorado Anschutz Medical Campus, Aurora CO

T.D.B is with Department of Pediatrics (Critical Care Medicine), University of Colorado Anschutz Medical Campus, Aurora CO

S.P is with Department of Neurology, Columbia University Irving Medical Center, New York-Presbyterian Hostpital, New York, NY

S.P. and D.J.A are with Department of Biomedical Informatics, Columbia University Irving Medical Center, New York-Presbyterian Hostpital, New York, NY

B.F is with Department of Neurology and Rehabilitation Medicine, University of Cincinnati, Cincinnati, OH

We acknowledge National Institutes of Health R01s LM006910 "Discovering and applying knowledge in clinical databases," and "Mechanistic machine learning," LM012734 to DJA, National Science Foundation (NSF) Graduate Research Fellowship DGE-1938058_Briggs to JKB

We thank the following TRACK-TBI Investigators: Neeraj Badjatia, MD, University of Maryland; Ramesh Grandhi, MD MS, University of Utah; Michael McCrea, PhD, Medical College of Wisconsin; Randall Merchant, PhD, Virginia Commonwealth University; Laura B. Ngwenya, MD, PhD, University of Cincinnati; Claudia Robertson, MD, Baylor College of Medicine; David Schnyer, PhD, UT Austin; John K. Yue, MD, University of California, San Francisco

I. Introduction

Secondary insults following traumatic brain injury (TBI) or cerebral vascular injury are often caused by ischemic events or acute underperfusion of the brain. Cerebral perfusion, or cerebral blood flow (CBF), is driven by the cerebral vascular resistance (CVR) and cerebral perfusion pressure (CPP), the pressure gradient formed between mean intracranial pressure (mICP) and mean arterial blood pressure (mABP) (equation 1). Therefore, to prevent secondary injuries, current clinical guidelines recommend targeting ICP to below 20-25 mmHg [1]. However, a precision medicine approach may be possible by targeting the state of the patient's vasculature. In particular, cerebral autoregulation (CA) is an intrinsic mechanism of the cerebral vasculature, which maintains adequate cerebral blood flow (CBF) over large pressure gradients by altering cerebral vascular resistance[2], [3]. CA can be impaired in injured patients. Retrospective studies have shown that patients have better functional outcomes when their CPP is close to a value that optimizes CA, called CPPopt[4], [5]. Therefore, patients may benefit from a CA-guided clinical management approach, such as CPPopt-guided therapy[6], [7]. CA function can be estimated using a variety of metrics, including transfer function analysis and the pressure reactivity index (PRx)[3], [4], [8]. Still, PRx is typically used in CPPopt-guided therapy. Recent clinical trials are moving CPPopt-guided treatment closer to becoming a new standard of care[9], [10]. However, the parameters used to calculate PRx can be variable in the literature (See Table 1), motivating investigation into how robust PRx is to methodological choices. This question is essential for comparing results from different manuscripts and raw PRx values across patients.

$$CBF = \frac{CPP}{CVR} = \frac{mABP - mICP}{CVR} \tag{1}$$

In general, cerebral autoregulation describes the observation that when CPP is below some threshold, called the lower limit of autoregulation, the relationship between CPP and CBF is linear (i.e., CVR is constant). Above the lower limit of autoregulation, there is no relationship between CPP and CBF in healthy patients (i.e., CVR changes to accommodate the changing pressure). Finally, above another threshold, called the upper limit of autoregulation, the relationship between CPP and CBF becomes linear again. Recent studies have questioned the exact details of CA, implicating that there may be more than two limits of autoregulation[3], [11], [12]; however, the general phenomenon is consistent across experimental

paradigms. Therefore, beyond the limits of autoregulation, there should be a strong correlation between ABP and CBF and a very weak correlation between ABP and CBF within the 'plateau' region of the autoregulation curve.

The challenge of patient-specific CA-guided clinical decision-making is how to quantify CA function. By the definition of CA given previously, CA should be measured by comparing CBF with CPP. However, this presents data challenges as CBF is rarely measured continuously[13]. The more common approach, also used in PRx, is to consider that CBF contributes to cerebral blood volume, and via the Monro Kellie doctrine[14], cerebral blood volume is transferred non-linearly into ICP. Using this assumption, PRx attempts to quantify CA by calculating the Pearson correlation coefficient between ABP and ICP. The more positively correlated the relation, the more impaired cerebral autoregulation is interpreted to be, provided CPP is in the autoregulatory range.

Multiple studies before the creation of PRx [15], [16] showed that CA does not act on frequencies as fast as heart rate or respiration[17]. Therefore, when PRx was created, the effect of these frequencies was removed by taking the 5-second moving average of both ABP and ICP signals (Fig 1a.) and then calculating the Pearson correlation coefficient of 40 consecutive samples between the averaged ICP and ABP values (Fig 1b,c)[8]. In statistics and data science, a hyperparameter is a parameter value chosen *a priori* which defines the algorithm or estimator behavior [18], [19]. Therefore, the width of averaging and correlation windows are hyperparameters in the PRx calculation. These exact hyperparameters used are variables in the literature. Table I shows some common hyperparameter choices.

Averaging Window (seconds)	*Number of Samples For Correlation*
10	40[20]
10	*30* (most common[21])[22]–[29]
5	40[8], [30]–[33]
15	30[34]*
6	40[4], [35], [36]

TABLE I
COMMON HYPERPARAMETERS USED TO CALCULATE PRX

The purpose of this manuscript is twofold. *First, we investigate the robustness and uncertainty of PRx calculation across hyperparameters and patients to provide a recommended hyperparameter set using the current methodology. Second, to test the hypothesis that an alternative, personalized parameterization of the PRx methodology accounting for the patient's heart rate will provide a more robust and stable estimation of CA.* We begin by calculating PRx in patient data using many different hyperparameters. It is currently not possible to validate PRx or CPPopt on clinical data because there is no direct measurement of the physiology underlying CA. Therefore, to quantify PRx error, we create physiologically informed simulated data. We find that PRx is sensitive to hyperparameter choices, and this sensitivity is patient specific, indicating that there may be ways to make PRx more robust by personalizing the methodology based on patient state. Finally, we show a simple modification to the PRx algorithm can significantly decrease PRx error, hyperparameter sensitivity, and measurement uncertainty.

II. METHODS

Data

Patient Data Patient data was taken from patients enrolled in the Transforming Research and Clinical Knowledge in Traumatic Brain Injury (TRACK-TBI) study[37], a prospective, multicenter study of patients with traumatic brain injury. Written informed consent was obtained and the study was approved by the institutional review boards of enrolling sites. For this investigation, we included patients undergoing multimodality monitoring from a single center within the TRACK-TBI study to ensure standardized physiologic measurements and clinical practice. However, the entire TRACK-TBI cohort was used for rescaling synthetic data. Patient demographics are given in Table II.

Data from 11 patients were extracted and segmented into four-hour windows. Four hours is the time recommended to calculate a target cerebral perfusion pressure (CPPopt)[32]. Windows were chosen to analyze if there was a four-hour window for which missing or erroneous data made up less than 10% of the window. Erroneous data was defined as ABP $> 400mmHg$ or $< 0mmHg$ and ICP $> 100mmHg$ or $< 0mmHg$. All erroneous data were set to null. Segments of erroneous data less than 1 second were filled through linear interpolation. The averaging scheme was left null during these time points for larger gaps and was therefore not included in the correlation.

Simulated Data It is not currently possible to validate which hyperparameter would give the correct PRx on patient data or calculate the error in PRx estimation. To quantify error, we created simulated data based on physiologically relevant signals (Fig. 2). Figure 2 shows a graphical description of simulated data creation. We created 200 simulated datasets, each containing ABP and ICP for the three CA phenotypes; "Functional CA", "Impaired CA", and "Absent CA", resulting in 600 example time series, based on the hypothesis that as CA becomes impaired, slower frequencies are translated from ABP to ICP[25], [38], [39].

First, five different waveforms were created over four hours of $125Hz$ resolution data (Figure 2.1). These waveforms were based on frequencies present in documented patient waveforms, including heart rate and respiration, which are present in both ABP and ICP; B-waves, which are present only in ICP and represent processes in ICP independent of ABP; and two random waves, which are meant to emulate random external changes in ABP or ICP (Table III). Care was taken such that these frequencies were not harmonics with each other. From these base frequencies, we created three ICP waveforms (Figure 2.2a). In functional CA, ICP should

*Howells recommends using 15-50 second averages but does not use any correlation window. For some consistency, we chose correlations that would result in the same amount of data captured in [25], [26](5 minutes)

†All data reported as mean+/-standard deviation, median [interquartile range], or proportion (%) as appropriate

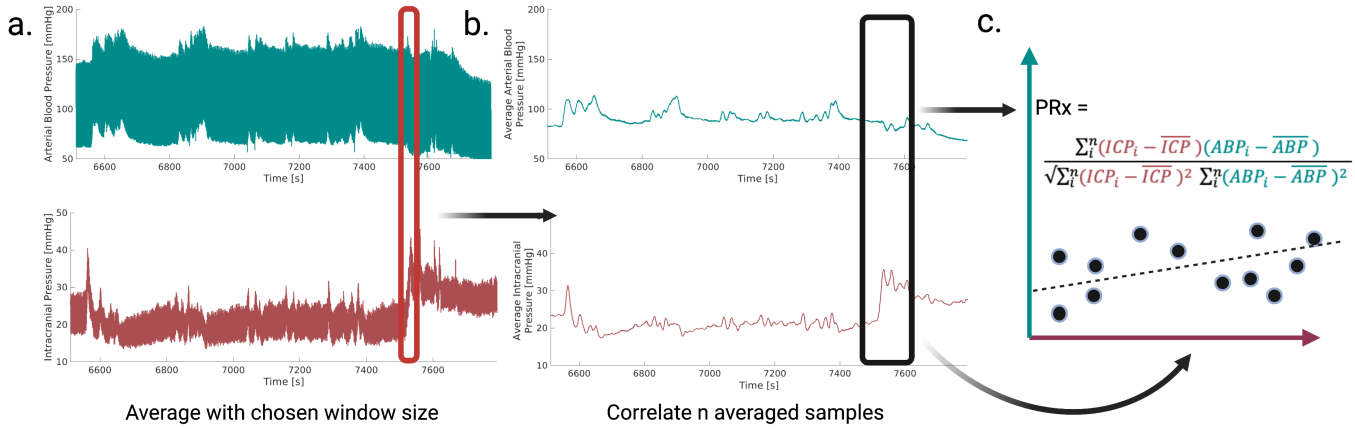

Fig. 1. Algorithm for calculating PRx. a: ABP (blue) and ICP (red) are averaged over a non-overlapping averaging window. b: n number of these averaged samples are collected, and the Pearson correlation coefficient is calculated (c) on a 4/5 overlap sliding window.

Variable†	*TRACK-TBI Physiology Cohort (UCMC), n=11*
Demographics	
Age, years	41.8±16.5
Sex, male	9 (82)
Injury Characteristics	
- Motor Vehicle Traffic Accident	6 (55)
- Fall	4 (36)
- Other	1 (1)
Time from Injury to Admission, hours	1 [0.7-1.5]
Admission GCS	3 [3-5]
Admission GCS Motor Subscore	1 [1-3]
Admission pupils, one or neither reacting	7 (64)
Injury Severity Score	25.5± 9.1
Patients Requiring Decompressive Hemicraniectomy	6 (55)
Monitoring Data	
Time from Injury to Moberg CNS Data, hours	7.3 [6.0-16.5]
Duration of Available Moberg CNS Data, hours	39.5 [32.2-100.7]
ICP Monitoring	11 (100)
Time from Injury to ICP Monitoring, hours	6.5 [5.7-11.6]
ICP Monitor Type	
- Parenchymal Monitor	9 (82)
- External Ventricular Drainage Catheter	
- Both	2 (18)
Outcome	
Hospital Length of Stay, days	15.1 [14.2-22.3]
In-Hospital Mortality	6 (55)
6-Month Mortality	8 (73)
6-Month Glasgow Outcome Scale-Extended	1 [1-2]

TABLE II

PATIENT CHARACTERISTICS AND MONITORING DATA. INJURY WAS CLOSED FOR ALL PATIENTS. ALL PATIENTS HAD MULTIMODAL MONITORING, INCLUDING ICP WAVEFORMS, EEG, AND PBTO2.

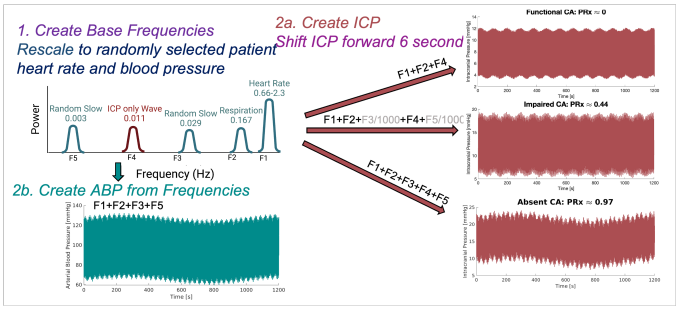

Fig. 2. Graphical depiction of the creation of simulated data set. Step 1 shows the power spectrum of the six base frequencies (Table III) used to create ICP and ABP. Blue indicates a representative ABP waveform. In each ABP waveform, the heartrate frequency was randomly selected between 40-140 bpm and was scaled to match the amplitude of a randomly selected patient from the TRACK-TBI dataset. Red indicates three ICP waveforms created from combinations of the base frequencies. Three CA phenotypes were created: Functional CA, Impaired Ca, and Absent CA. The frequencies used to create each ICP waveform are given above the red arrows

Signal Name	*Physiologic Interpretation*	*Rate or Period*	
$F1$	Heart Rate	40-140 beats per minute	Scaled in frequency and amplitude to match randomly selected patient from UC Cincinnati dataset
$F2$	Respiration	10 breaths per minute	
$F3$	Random	30 second period	Meant to emulate random external changes to the patient, slow enough for CA to buffer[17], [39]
$F4$	Waves only present in ICP	90 second period	Found only in ICP[40]
$F5$	Random	16-minute period	Meant to emulate slow random external changes to the patient

TABLE III

PHYSIOLOGICALLY RELEVANT FREQUENCIES USED IN SIMULATED DATA

reflect heart rate, respiration, and B-waves[8], [25], [38], [41]. Therefore, $ICP = F1 + F2 + F4$. Impaired CA passes faster frequencies into ICP and allows only decreasing portions of the slower waves to pass through[25], [38], [39]. Therefore, $ICP = F1 + F2 + F3/1000 + F4 + F5/1000$. 1000 was chosen to minimize the impact that the frequencies had on ICP and the correlation coefficient. In absent CA, PRx assumes that most or all of the frequencies present in ABP will be reflected in ICP. Therefore, $ICP = F1+F2+F3+F4+F5$. ABP was created by summing all physiologically relevant frequencies except for B-Waves (F4), representing oscillations found in ICP but not ABP. We then shifted all ICP waveforms by 6.8 seconds as some of the ICP waveforms are caused by traveling ABP waves, causing ICP to be lagged behind ABP[42]. ICP and ABP were then rescaled according to physiological values for each dataset. To obtain physiological rescaling values, we extracted full timecourses of ABP and ICP from all patients within the TrackTBI dataset. We fit a gamma distribution to each patient's ICP and ABP data using Matlab's *fitdist* function. For each dataset, we randomly selected a representative patient and rescaled ICP and ABP according to that patient's distribution. As CA is one of many factors contributing to ICP value, we rescaled all three ICP waveforms to the same amplitude.

PRx is meant to capture the correlation between ABP and ICP after removing effects of heart rate and respiration, 'True' PRx was defined as the correlation coefficient over the whole waveform between $F3$ and $F5$ in ABP and all frequencies slower than $F3$ in ICP.

Analysis

Calculating PRx To test the sensitivity of PRx estimation to hyperparameters, we calculated PRx for every combination of averaging windows between 1 and 30 seconds and every correlation window between 2 and 65 averaged samples. We chose this broad range to capture every methodology presented in the literature. According to standard methods, averaging windows did not overlap [25], correlation windows are calculated so that the number of samples overlaps by 4/5. All calculations were done in Matlab and are publically available at: https://github.com/jenniferkbriggs/PRx. Unless otherwise noted, the reported PRx value is the median PRx across the four-hour dataset. Since the PRx calculation has high variance (noisy), we chose to use the median as it is more robust to noise than the mean.

Calculating Empirical Estimator Bias: To calculate empirical estimator bias from patient data, we first extracted the PRx estimation for each patient using the five common PRx hyperparameters outlined in table I. Because each method is based on different time windows, the time over which each PRx value is computed was slightly different. The output of each PRx method was then interpolated to compare values directly. The empirical estimator bias per patient was calculated according to equations 5 and 3.

$$\text{Empirical Estimator Bias}_j = \frac{1}{T_N}\sum_{n=1}^{T_N}(\widehat{PRx}_{t_n,j} - \overline{PRx_{t_n}}) \tag{2}$$

At each time point, $PRx_{t_n,j}$ is averaged over PRx estimation from a wide range of common hyperparameters (averaging windows between 5-20 seconds and correlation windows between 20-50 seconds) to define $\bar{PRx}$, which is used as a center point for bias calculations.

$$\overline{PRx(t_n)} = \frac{1}{J}\sum_{j=1}^{J} PRx(t_n)_j \tag{3}$$

t_n is the time point, T_N is the total time, j is the hyperparameter pair, J is the total number of hyperparameters analyzed, and $\widehat{PRx}$ is the estimated PRx for hyperparameter j and time t_n.

In simulated data where there is a ground truth PRx value, estimator bias is given by equation 5 but $\overline{PRx_{t_n}}$ is replaced with the predefined PRx value.

Calculating Sensitivity: Sensitivity was calculated by iterating through every hyperparameter pair and calculating the percent difference between the PRx value estimated using the hyperparameter pair and the PRx value estimated using the hyperparameter pairs by averaging with ± 1 second or correlating ± 1 given by equation4. Sensitivity can be interpreted as the average percent change in PRx value given a small change in hyperparameter choice.

$$\begin{aligned}\text{Sensitivity} = \frac{1}{4N}\sum_{i=1}^{N}\frac{PRx(n+1) - PRx(n)}{PRx(n)} \\ + \frac{PRx(n-1) - PRx(n)}{PRx(n)} + \frac{PRx(n+Av) - PRx(n)}{PRx(n)} \\ + \frac{PRx(n-Av) - PRx(n)}{PRx(n)}\end{aligned} \tag{4}$$

N is the number of unique hyperparameter pairs and $PRx(n)$ is the PRx for a given hyperparameter, and Av is the number of averaging windows, allowing us to index into a 2D matrix using one number.

The range of PRx values was calculated as the difference between the PRx estimation from the hyperparameter with the largest median PRx value and the PRx estimation from the hyperparameter with the smallest median PRx value.

To quantify uncertainty or sensitivity as a percentage, we calculated Percent change $= \frac{x_2 - x_1}{x_1}$, where x_1 is the initial value and x_2 was the final value being compared.

Identifying Optimal Hyperparameters

Optimal hyperparameters were identified using both patient and simulated data. In patient data, the standard deviation (SD) of bias in PRx estimation was the standard deviation of the empirical estimator bias across the 21 datasets. We defined optimal thresholds for each of the four metrics as the lowest thresholds that yielded hyperparameters consistent with the other metrics. SD of bias in PRx for patient data had a threshold of 0.022, for simulated data 0.22, for average bias of PRx we used a threshold $|0.01|$ for patient data, and $|0.22|$ for simulated data.

The standard deviation of estimator bias over time was calculated by first interpolating PRx estimation from all hyperparameters using linear interpolation to match time points. Discrete-time empirical estimator bias was calculated as the difference between PRx from the hyperparameter and $\overline{PRx_{t_n}}$ defined previously. The standard deviation of the estimator bias over time was calculated as the standard deviation of the discrete-time empirical estimator bias over all datasets, where ($d \in D$) represents each dataset.

Standard Deviation of Empirical Estimator Bias$_j$

$$= SD([\widehat{PRx}_{t_n,j} - \overline{PRx_{t_n}}]_{d \in D}) \quad (5)$$

Statistical significance was calculated using a paired one-way ANOVA with multiple comparisons.

Heartbeat identification and PRx calculation

To investigate our hypothesis that personalizing the PRx algorithm by averaging over patient heartbeat would provide a more robust and stable estimation of CA, we first identified all heartbeats in patient signals. Heartbeats in patients and simulated data were found using a sliding peak identification method on ABP. Data were segmented into one-minute and one-second windows with one-second overlap. A heartbeat is defined from the beginning of systole to the end of diastole. In each window, the beginning of each systolic phase was identified using Matlab's *findpeaks* function of the inverted ABP segment. To ensure the dicrotic notch was not mistaken as a peak, the minimum peak prominence was set to be half of the range of max ABP to min ABP during the minute window. For sections of missing data, heartbeats were imputed as the average heart rate of the previous minute-long section. PRx was calculated as previously, but averaging windows were calculated using a given number of heartbeats rather than seconds.

All statistical tests are two-sided paired Student's t-tests.

III. Results

PRx is Sensitive to Hyperparameters

Using data from 11 traumatic brain injury (TBI) patients at the University of Cincinnati, we segmented the patient data into four-hour segments resulting in 21 datasets. To validate our PRx calculation, we plotted the PRx estimation present in the clinical dataset against our PRx estimation with hyperparameters 10 seconds average and 30 samples of correlation (Supplemental Fig. 1). 3 out of 21 datasets did not contain PRx estimation and were excluded from the validation step. The average lagged correlation for each dataset was 0.89, with a standard deviation of 0.05 and an average lag of -0.0160 seconds. We lagged the correlation because the PRx calculation is sensitive to the initial starting time and we did not have information on what time the PRx calculation was started in the clinical dataset. The primary source of error was this time lag and differences in posterior quality control and artifact removal not available in the operational clinical environment where clinical PRx was initially calculated. Given these differences, this correlation is strong enough to conclude that our PRx estimation is valid.

We first compared PRx estimation resulting from the five common hyperparameters given in Table I. Hyperparameter with ten-second averaging windows and 40 sample correlation had the lowest average empirical estimator bias and smallest uncertainty between the five common hyperparameters (Fig. 3a). Overall, shorter averaging windows (5-6 seconds) were positively biased (hyperparameter overestimates PRx compared to the mean), whereas longer averaging windows were negatively biased (hyperparameter underestimates PRx compared to the mean). These results indicate that across 21 datasets, PRx is sensitive to hyperparameter choices.

Because CPPopt is calculated by finding the CPP value for which PRx is minimized, we wanted to investigate whether the time and corresponding CPP for which PRx is minimized is also sensitive to hyperparameter choices, thereby directly impacting the CPPopt calculation used to guide clinical decision-making. Fig. 3b shows the one-hour window around the time when PRx was minimized for three representative patients (patient numbers correspond to patient numbers in Fig. 3b). For patient **i**, PRx is minimized at a similar value for the same time for all hyperparameters. This represents the ideal situation. For patient **iii**, the value of PRx minimization ranges between very good CA (PRx = -0.6) for the three hyperparameters with long averaging windows (10-15 sec) and absent CA (PRx = 0.25) for the two hyperparameters with short averaging windows (5-6 sec), agreeing with our previous findings that different hyperparameters lead to varying interpretation of CA function. In patient **v**, PRx is minimized at different times, ranging across 30 minutes. In this patient, we plotted the CPP (left y-axis in blue bars) at the times when PRx was minimized. Depending on the hyperparameter, optimal CPP ranged from 50 - 59 mmHg. These results indicate that the value of PRx and the time for which PRx reaches a minimum value are both sensitive to hyperparameter choices.

Sensitivity to Hyperparameters is Heterogenous Across Patients

While our results indicate that PRx is not robust to hyperparameter choices, if the behavior of the sensitivity is consistent across patients, one can quantify the bias and control for it. Therefore, we chose to quantify the sensitivity for each patient. Fig. 3c shows contour plots of the estimated temporal median PRx over the hyperparameter combinations for five individual patients. The different colors on a single contour plot, corresponding to different PRx estimations, indicate that PRx is sensitive to hyperparameters, as shown previously. The different types of contours (e.g., horizontal (ii) or diagonal and curved (iv and v)) indicate that the extent and behavior of PRx sensitivity are heterogeneous across patients. For example, in patient ii, using 18 sample correlations and 5, 6, or 7-second averaging windows results in median PRx values of 0.31, 0.28, and 0.17, respectively. This means that changing averaging window will change the PRx estimation by up to 82%.

To quantify sensitivity further, we defined the extent of PRx uncertainty as the range of PRx values for the five common methods. The difference in PRx estimation across the five common hyperparameters ranged was 0.054 for the least

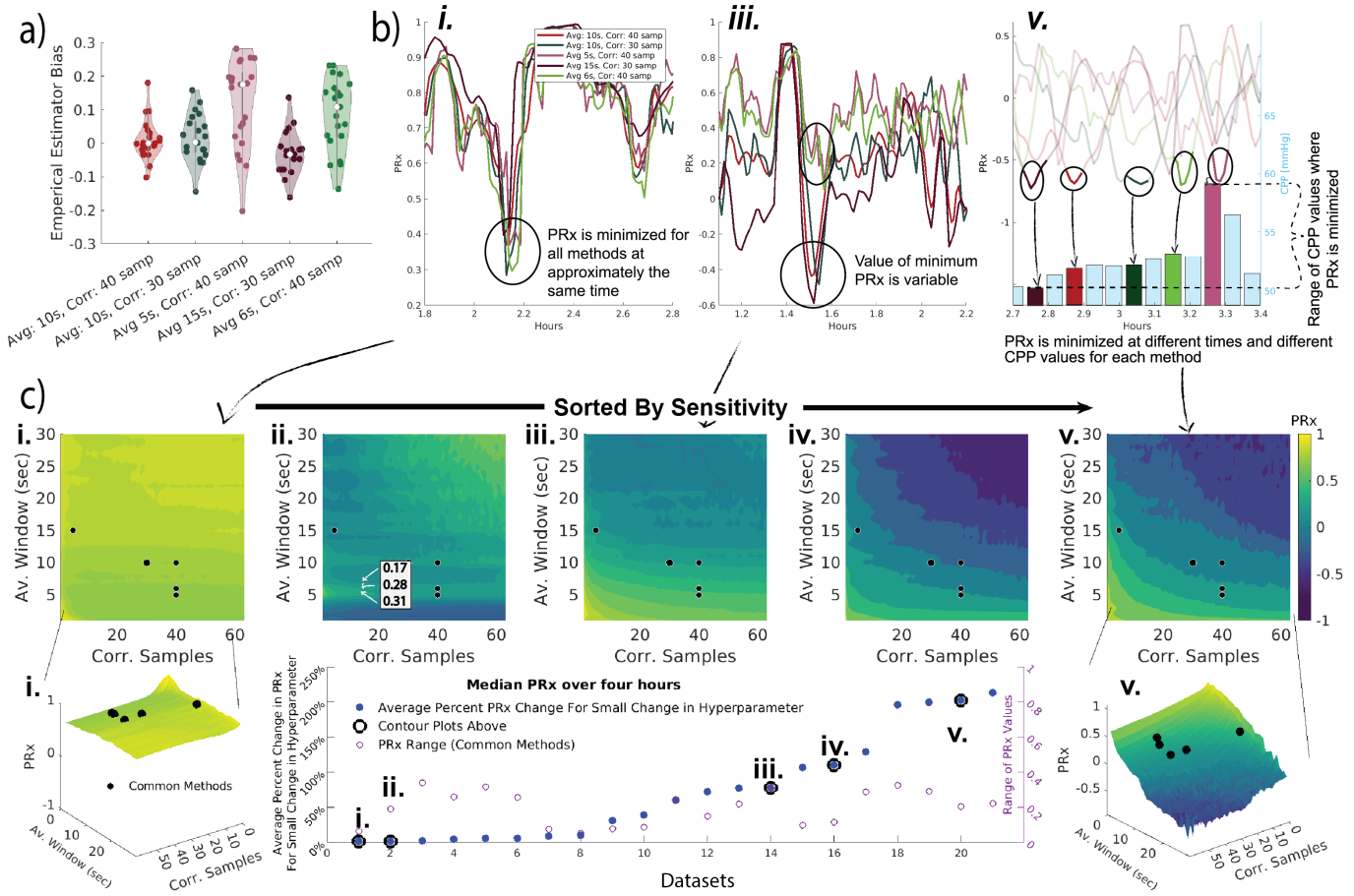

Fig. 3. PRx is sensitive to hyperparameters. a) Empirical estimator bias of PRx estimation using the most common hyperparameters. Dots indicate single patient datasets. b) Time courses of PRx estimation using the most common hyperparameters for three representative patients, corresponding to those in c. Black circles indicate when PRx was minimized for each patient over four hours, highlighting that PRx minimization is sensitive to hyperparameter choices. In patient **v**, PRx is shown on the left y-axis and CPP for the corresponding time is shown on the right axis. CPP bars are colored according to the corresponding hyperparameter where PRx was minimized. Dashed line indicates the range of CPP values where PRx was minimized. c) Quantified sensitivity to all hyperparameters analyzed. Contour plots show results from five representative patients. Differences in contour plot topography indicate that PRx sensitivity is patient-dependent. The scatter plot shows sensitivity for all patients, with black circles outlining five representative patients whose contour plots are shown.

sensitive patient and 0.34 for the most sensitive patient (3c right y-axis of scatter plot). Considering PRx can be between -1 and 1, this corresponds to an uncertainty in PRx between $2.5\% - 17\%$ of the possible PRx values. If we calculate the difference in PRx across all hyperparameters analyzed, PRx estimation had a minimum uncertainty of 0.32 and a maximum uncertainty of 1.57, corresponding to an uncertainty 16% - 79% across the possible PRx values (Supp. Fig.2). We also quantify the global sensitivity at a granular level using the average percent change in PRx estimation given a small change in hyperparameter (1-second different averaging window, one sample different correlation window)(3c left y-axis of scatter plot). Results range from $1.6\% - 213\%$ depending on the patient. Indicating that the influence of a small change of hyperparameters could make a large change in PRx estimation, and the amount of change in PRx is heterogeneous across patients. Together, these results show that PRx is sensitive to hyperparameters, and the sensitivity of PRx is heterogenous across patients. Therefore, a single hyperparameter choice can result in a different error for different patients, and a patient-specific hyperparameter choice may be necessary for ensuring the robustness of PRx.

PRx Error in Simulated Data

We then used the simulated data to evaluate the error of PRx estimation. To quantify hyperparameter-induced error and bias compared to the true PRx value, we calculated PRx for all hyperparameter choices (as in patient data) for 600 datasets of simulated data. In general, all hyperparameters were least accurate for impaired CA and most accurate for functioning CA (Fig. 4a). As in patient data, shorter averaging windows underestimated PRx, and larger ones overestimated PRx compared to common hyperparameters. However, in the simulated data, PRx was most accurate for longer averaging windows because of this overestimation. In agreement with the patient data, larger averaging windows decreased uncertainty.

Identifying Optimal Hyperparameters Using Patient and Simulated Data.

Despite the possible usefulness of a personalized hyperparameter choice, we first chose to investigate the optimal

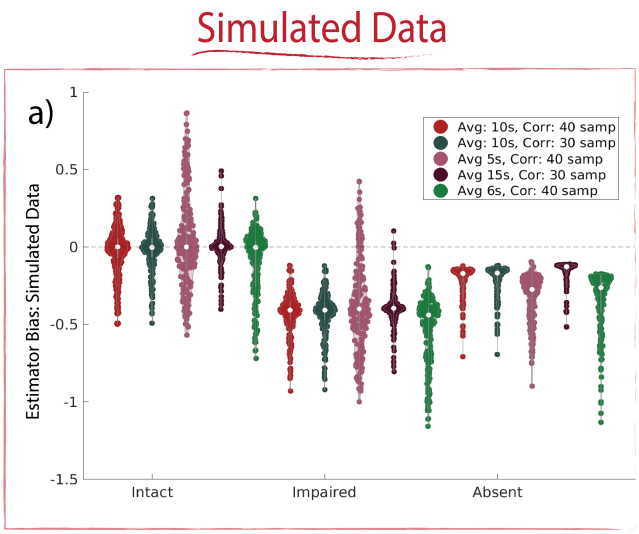

Fig. 4. PRx error in simulated data. a) Estimator bias for intact (left), impaired (middle), and absent (right) CA for five common hyperparameters.

hyperparameters for the current non-personalized PRx algorithms. We identified the hyperparameter pairs which minimized the standard deviation (SD) of estimator bias (or empirical estimator bias) and average bias for simulated and patient data, respectively (fig 5a-d). The hyperparameters which minimized standard deviation and bias in patient and simulated data were averaging windows between 9-10 seconds and correlation windows between 35-55 samples. The 10 second averaging 40 sample correlation hyperparameter pair was the only hyperparameter pair in the Table I that fit within this range. Visually, the 10 seconds and 40 sample hyperparameter decreased uncertainty, or noise, over time (fig 5e). This hyperparameter significantly decreased the standard deviation of empirical estimator bias over time compared to all other common hyperparameters.

Novel Heartrate Specific Methodology Reduces Error, Sensitivity to Hyperparameters, and Uncertainty in PRx Estimation

To test the hypothesis that personalizing PRx by heart rate will reduce sensitivity and bias, we first identified all heartbeats in the patient and simulated data (Fig. 6a). We then analyze how heart rate impacted PRx error in simulated data. There is a nonlinear relationship between heart rate and error in the simulated dataset (Fig. 6b), with heart rate having the greatest effect in the impaired and absent CA cases and the least effect for intact CA. This relationship implies there may be a way to reduce patient-specific errors by personalizing PRx to heart rate.

Therefore, we chose to try personalizing the PRx algorithm by averaging over heartbeat rather than seconds. For example, if the hyperparameter pair was averaging over ten seconds and correlating over 30 samples, we instead averaged over ten heartbeats and correlated over 30 samples. This method would presumably minimize the impact of intrapatient heart rate variability and interpatient average heartbeat differences. After identifying all heartbeats, we repeated the calculated PRx for all hyperparameters in both patient and simulated data averaging over a given number of heartbeats rather than seconds.

In simulated data, the heartbeat averaging method decreased PRx estimator bias uncertainty and improved average estimator bias for absent CA (Fig. 6c). In the 21 patient datasets analyzed, PRx estimation was different between the two averaging methodologies (Fig. 6d.).For PRx > 0.4, the heartbeat averaging methodology tended to estimate PRx to be larger than the estimate from the seconds averaging methodology. Our previous results in simulated data (Fig. 4a) indicate that the seconds averaging method underestimates PRx for patients with impaired and absent CA.

To further quantify the effect of this heartbeat method, we compared the sensitivity of PRx to different hyperparameters (Fig. 6e) and the uncertainty in the PRx estimation over time for the most common hyperparameter pair: average over ten seconds or heartbeats and correlated over 30 samples (Fig. 4f). The heartbeat averaging method significantly reduced PRx sensitivity to methods ($P = 0.0114$) and uncertainty of PRx over time ($P < 0.0001$) compared to the averaging method. The heartbeat averaging method did not notably impact PRx computation time. These results indicate that PRx estimation can be made more robust by averaging over heartbeats rather than seconds.

IV. Discussion

The pressure reactivity index (PRx) is a clinically important metric for evaluating cerebral autoregulation (CA) function. PRx and CPPopt are becoming increasingly common in the clinical workflow for treating patients with neurovascular and neurological injuries. PRx is calculated using two hyperparameters: averaging windows and correlation windows. The importance of these hyperparameters remains an open question. The objective of this study was to quantify how sensitive PRx is to hyperparameters and investigate simple methodologies for improving the robustness of PRx. We found that PRx is sensitive to hyperparameters, and this sensitivity is patient-dependent. As our sample size was relatively small, our results are likely a conservative estimate of the possible bias and sensitivity of PRx, because the prevalence of outliers generally increases as sample size increases. Typically, PRx > 0.25 is interpreted as impaired CA and thought to predict a higher risk of mortality[29], [43], while PRx value < 0 is interpreted as intact CA. Therefore, the critical threshold between 'good' PRx and 'bad' is ≈ 0.25.

We chose to analyze the sensitivity of PRx in a few different ways, each of which has different implications for the PRx interpretation. If the empirical estimator bias (Fig. 3a) for a given hyperparameter was relatively consistent across patients, one could easily compare hyperparameters while taking this bias into account. However, our data show that the bias is patient and hyperparameter specific. There is an uncertainty in hyperparameter bias of 0.3 which is larger than the critical threshold of PRx, indicating that values of PRx may have different interpretations across studies that use different hyperparameters. The range of possible PRx values allows

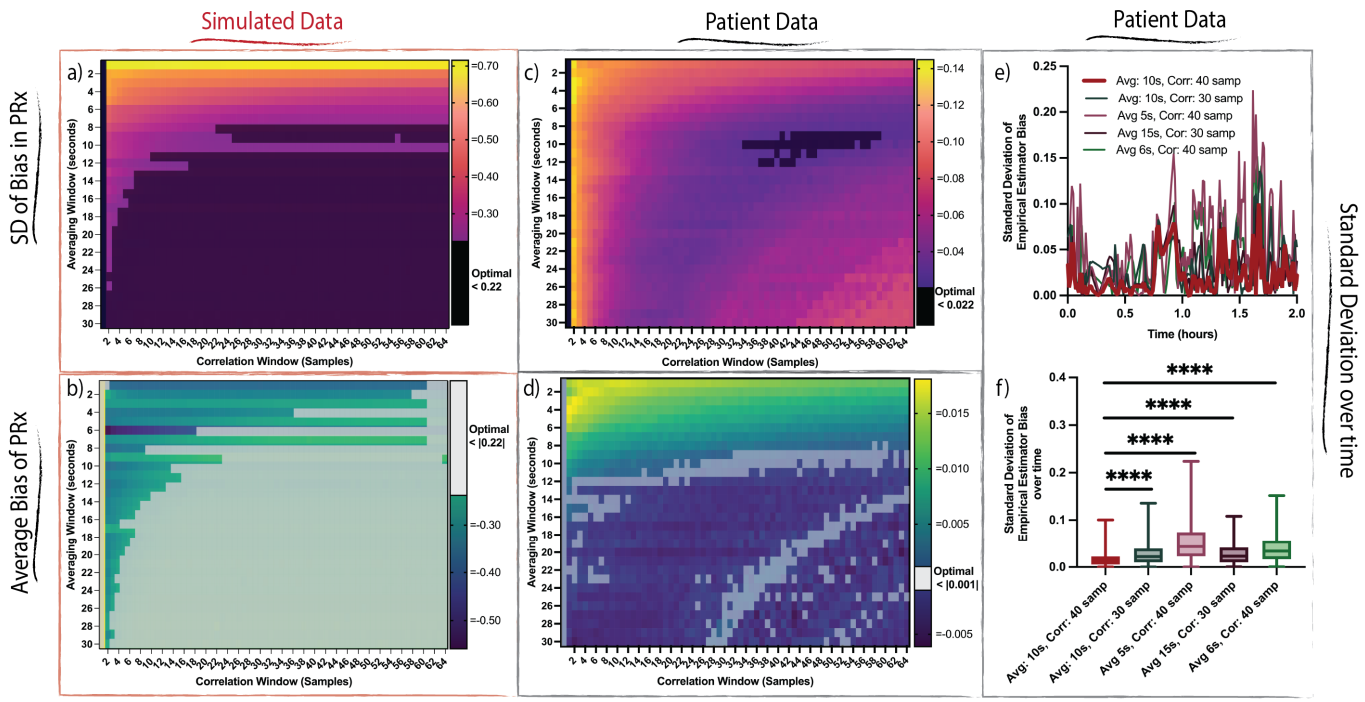

Fig. 5. Bias in PRx estimation of all hyperparameters for simulated and patient data. a) Contour plots showing standard deviation (SD) of estimator bias in PRx for simulated data. Black hyperparameters indicate hyperparameters that minimized the SD of bias for these data. b) Contour plots showing average bias in simulated data. White indicates hyperparameters that minimized bias. c) As in a but for patient data. d) As in c but for patient data. e) One hour time series of the standard deviation of empirical estimator bias for the five common hyperparameters. Averaging window of 10 seconds and correlation window of 40 samples lies within the optimal hyperparameter range and is bolded. f) Comparison between the standard deviation of empirical estimator bias for each time point. Averaging window of 10 seconds and correlation window of 40 samples had significantly smaller bias ($p < \mathbf{0.0001}$) compared to other common hyperparameters. Analysis was paired one-way ANOVA with multiple comparisons.

us to quantify how sensitive PRx is to hyperparameters. In our cohort, the range of median PRx across the five common hyperparameters was between 0.054 and 0.34. This high level of hyperparameter influence (compared to the critical threshold of PRx) has important implications for clinical decision-making.

It is not likely that a monitor would change hyperparameters throughout a patient's stay, so one may argue that the relative PRx value (relative to the patient) would be robust to this hyperparameter sensitivity. While this is partly true, changes in hyperparameters can also be interpreted as missing data. For example, in figure 3c patient ii, missing one second of data per averaging window results in a change of median PRx estimation from 0.17 to 0.28, which crosses the critical threshold. Changes in correlation samples can be interpreted as missing a 5-30 second piece of data within a longer time. Therefore, because of the prevalence of missing data in clinical settings, the sensitivity of PRx to hyperparameters may be influential even when the algorithm is calculated using one hyperparameter pair.

Current clinical decision-making targets are not based on raw PRx values but rather on the CPP for which PRx is minimized (CPPopt). Decisions based on the wrong hyperparameter could guide decisions that cause over or underperfusion of the patient. Our results indicate that the time and CPP for which PRx is minimized may be hyperparameter dependent. However, the fact that CPPopt is calculated using a parabolic fit and averaging of PRx over the four-hour epoch[32] may help remove some of this uncertainty.

A central challenge in the study of PRx is that it cannot be directly validated in critically ill patients. Compared to other CA metrics, PRx is a more successful predictor of mortality[44], and in animals, PRx was shown to be a good predictor of the lower limit of autoregulation (AUC = 0.795)[45], [46]. However, quantifying hyperparameter-dependent PRx error is not possible in patient data. Therefore, we created simulated data using assumptions underlying PRx (see methods) and physiologically relevant frequencies. While the interpretation of simulated data is always limited, creating our simulated data based on assumptions made in the PRx allows us to probe these assumptions and quantify error. In the simulated data, we find that patients with impaired CA have the least accurate PRx estimation compared to functional or absent. This is important because patients with impaired, but not completely absent PRx are likely those who will benefit most from CA-guided therapy, as those with intact CA should be able to regulate over large ranges of CPP, and by definition, there is no way to guide therapy based on where CA is most functional if CA is absent.

Using synthetic and patient data, we concluded that the optimal hyperparameters are averaging windows between 9-10 seconds and correlation windows between 40-44 samples. This recommendation is in line with previous experimental studies[23], [34]. From a data science perspective, it makes sense that the optimal averaging window is medium in length. Increasing the number of data points used for averaging will

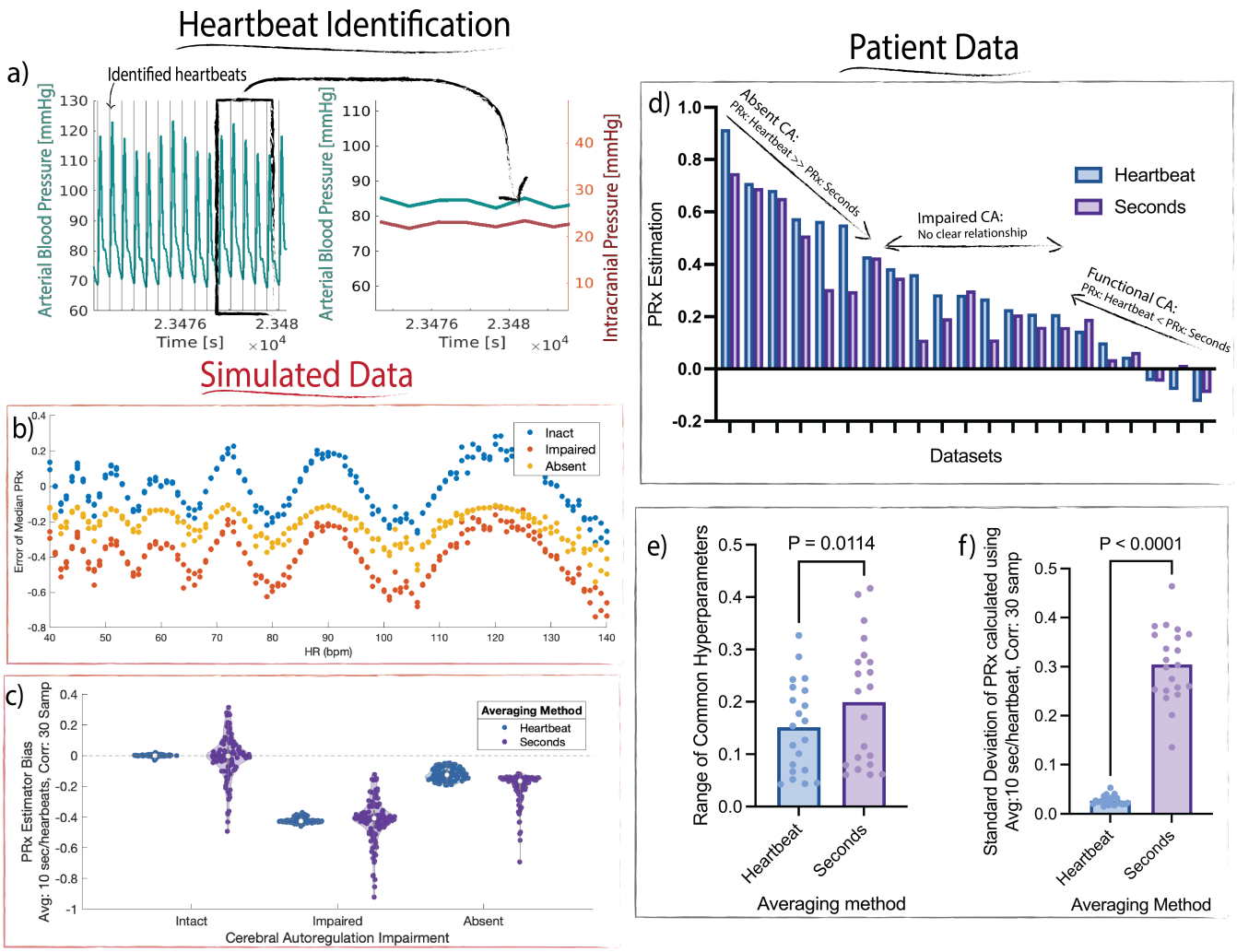

Fig. 6. Comparison between traditional PRx calculation and new heartbeat-specific averaging. a) Representative ABP signal with black lines indicating heartbeat start times (left). ABP (teal) and ICP (red) are averaged over a given number of these heartbeats (right). b) Dependence of median PRx error on heart rate for intact (blue), impaired (red), and absent (yellow) CA in simulated data. c) PRx estimator bias in simulated data comparing heartbeat (blue) and seconds (traditional, purple) averaging methods. d) Sorted median PRx in patient data for the heartbeat (blue) and seconds (purple) averaging methods. e) Range of PRx estimation amongst five common hyperparameters. Dots indicate each dataset. f) Standard deviation of PRx over a four-hour window calculated by averaging over 10 seconds (purple) or heartbeats (blue) and correlating over 30 samples. P-values in d and e are two-tailed paired students' t-tests.

decrease bias. This is likely why larger averaging windows decreased bias and uncertainty in both synthetic and patient data. However, according to the sampling theorem, any frequency faster than half the width of the averaging window will be smoothed over and therefore not be resolved[47]. Therefore, too long of an averaging window will not resolve essential frequencies in CA and, therefore, will not be able to distinguish between functional, impaired, and intact frequencies, which may be the case when using indices such as long-PRx [48].

We have recommended a set of optimal hyperparameters using the current PRx methodology. However, our data suggest that PRx sensitivity is patient-dependent (Fig. 3c.). Therefore, personalizing the PRx algorithm to the patient's state may further reduce error. Using simulated data, we found that heart rate was associated with error in PRx estimation. We found that personalizing the PRx estimation by averaging over heartbeats rather than seconds decreased bias, uncertainty in bias, uncertianty in PRx, and sensitivity of PRx estimation to hyperparameters patient and simulated data (Fig 6).

The fact that PRx is associated with heart rate also has important implications for using PRx in pediatric care, as the average heart rate varies strongly between children and adults. These facts motivated our investigation of a patient's heart rate-specific PRx methodology.

PRx is a valuable metric partly due to its simple and fast algorithm. By averaging over heartbeats, these benefits are maintained (as opposed to a more computationally expensive patient-specific method). We found that averaging over heartbeats significantly decreases uncertainty and bias in simulated data (Fig. 6b,d,e). This bias is not entirely removed, likely due to limitations in the simulated data and limitations of the PRx algorithm. In patient data, PRx from the heartbeat method was larger than standard PRx for patients with large PRx values, indicating absent CA. Therefore, the heartbeat

averaging method may reduce the bias found using simulated data, thereby increasing PRx estimation accuracy. Therefore, we conclude that averaging over heartbeats rather than seconds significantly decreases hyperparameter uncertainty and noise in PRx estimation and may decrease PRx estimation error.

V. Conclusion

The pressure reactivity index (PRx) is an important proxy for cerebral autoregulatory function and shows great promise in aiding clinical decision-making for neurologically ill patients. In this manuscript, we show that PRx is sensitive to methodological hyperparameters. This sensitivity is heterogenous across patients, partly due to differences in heart rate. Reducing this sensitivity is crucial for increasing the usefulness of PRx and CPPopt-guided clinical decision-making and is vital to investigrate for populations with different average heartrate, such as the pediatric population.

Recomendations Based on Findings

We conclude with two recommendations. In the current PRx algorithm, we recommend averaging windows between 9-10 seconds and correlation windows between 40-55 samples. These hyperparameters significantly decrease uncertainty in PRx compared to other common hyperparameters in patient data and decrease PRx bias for patient and simulated data. To further decrease error and make the PRx algorithm patient specific, we recommend averaging based on patient heart rate rather than seconds. The software for this new algorithm will be made publically available. This modification decreases uncertainty, sensitivity, and bias in the PRx calculation, allowing for greater reliability of PRx and its use in clinical decision-making.

References

[1] N. Stocchetti and A. I. Maas, "Traumatic intracranial hypertension," *New England Journal of Medicine*, vol. 370, no. 22, pp. 2121–2130, 2014.

[2] N. A. Lassen, "Cerebral blood flow and oxygen consumption in man," *Physiological reviews*, vol. 39, no. 2, pp. 183–238, 1959.

[3] J. A. Claassen, D. H. Thijssen, R. B. Panerai, and F. M. Faraci, "Regulation of cerebral blood flow in humans: Physiology and clinical implications of autoregulation," *Physiological reviews*, vol. 101, no. 4, pp. 1487–1559, 2021.

[4] L. A. Steiner, M. Czosnyka, S. K. Piechnik, *et al.*, "Continuous monitoring of cerebrovascular pressure reactivity allows determination of optimal cerebral perfusion pressure in patients with traumatic brain injury.," *Critical care medicine*, vol. 30, no. 4, pp. 733–738, 2002.

[5] J. Donnelly, M. Czosnyka, H. Adams, *et al.*, "Individualising thresholds of cerebral perfusion pressure using estimated limits of autoregulation," *Critical care medicine*, vol. 45, no. 9, p. 1464, 2017.

[6] A. I. Maas, D. K. Menon, P. D. Adelson, *et al.*, "Traumatic brain injury: Integrated approaches to improve prevention, clinical care, and research," *The Lancet Neurology*, vol. 16, no. 12, pp. 987–1048, 2017.

[7] N. Stocchetti, M. Carbonara, G. Citerio, *et al.*, "Severe traumatic brain injury: Targeted management in the intensive care unit," *The Lancet Neurology*, vol. 16, no. 6, pp. 452–464, 2017.

[8] M. Czosnyka, P. Smielewski, P. Kirkpatrick, R. J. Laing, D. Menon, and J. D. Pickard, "Continuous assessment of the cerebral vasomotor reactivity in head injury," *Neurosurgery*, vol. 41, no. 1, pp. 11–19, 1997, ISSN: 0148-396X.

[9] J. Tas, E. Beqiri, R. C. van Kaam, *et al.*, "Targeting autoregulation-guided cerebral perfusion pressure after traumatic brain injury (cogitate): A feasibility randomized controlled clinical trial," *Journal of Neurotrauma*, vol. 38, no. 20, pp. 2790–2800, 2021.

[10] E. Beqiri, P. Smielewski, C. Robba, *et al.*, "Feasibility of individualised severe traumatic brain injury management using an automated assessment of optimal cerebral perfusion pressure: The cogitate phase ii study protocol," *BMJ open*, vol. 9, no. 9, e030727, 2019.

[11] S. P. Klein, V. De Sloovere, G. Meyfroidt, and B. Depreitere, "Differential hemodynamic response of pial arterioles contributes to a quadriphasic cerebral autoregulation physiology," *Journal of the American Heart Association*, vol. 11, no. 1, e022943, 2022.

[12] P. Brassard, L. Labrecque, J. D. Smirl, *et al.*, "Losing the dogmatic view of cerebral autoregulation," *Physiological reports*, vol. 9, no. 15, e14982, 2021.

[13] J. Tas, M. Czosnyka, I. C. van der Horst, *et al.*, "Cerebral multimodality monitoring in adult neurocritical care patients with acute brain injury: A narrative review," *Frontiers in Physiology*, vol. 13, p. 2433, 2022.

[14] B. Mokri, "The monro–kellie hypothesis: Applications in csf volume depletion," *Neurology*, vol. 56, no. 12, pp. 1746–1748, 2001.

[15] G. Florence and J. Seylaz, "Rapid autoregulation of cerebral blood flow: A laser-doppler flowmetry study," *Journal of Cerebral Blood Flow & Metabolism*, vol. 12, no. 4, pp. 674–680, 1992.

[16] R. Aaslid, K.-F. Lindegaard, W. Sorteberg, and H. Nornes, "Cerebral autoregulation dynamics in humans.," *Stroke*, vol. 20, no. 1, pp. 45–52, 1989.

[17] C. D. Fraser III, K. M. Brady, C. J. Rhee, *et al.*, "The frequency response of cerebral autoregulation," *Journal of Applied Physiology*, vol. 115, no. 1, pp. 52–56, 2013.

[18] M. P. Deisenroth, A. A. Faisal, and C. S. Ong, *Mathematics for machine learning*. Cambridge University Press, 2020, ch. 8.1.

[19] D. S. Wilks, *Statistical methods in the atmospheric sciences*. Academic press, 2011, vol. 100, ch. 6.

[20] A. Akhondi-Asl, F. W. Vonberg, C. C. Au, and R. C. Tasker, "Meaning of intracranial pressure-to-blood pressure fisher-transformed pearson correlation–derived optimal cerebral perfusion pressure: Testing empiric utility

in a mechanistic model," *Critical care medicine*, vol. 46, no. 12, e1160, 2018.

[21] P. Smielewski, M. Czosnyka, L. Steiner, M. Belestri, S. Piechnik, and J. Pickard, "Icm+: Software for on-line analysis of bedside monitoring data after severe head trauma," in *Intracranial pressure and brain monitoring XII*, Springer, 2005, pp. 43–49.

[22] K. P. Budohoski, M. Czosnyka, N. de Riva, *et al.*, "The relationship between cerebral blood flow autoregulation and cerebrovascular pressure reactivity after traumatic brain injury," *Neurosurgery*, vol. 71, no. 3, pp. 652–661, 2012.

[23] K. M. Brady, J. K. Lee, K. K. Kibler, R. B. Easley, R. C. Koehler, and D. H. Shaffner, "Continuous measurement of autoregulation by spontaneous fluctuations in cerebral perfusion pressure: Comparison of 3 methods," *Stroke*, vol. 39, no. 9, pp. 2531–2537, 2008.

[24] P. Bijlenga, M. Czosnyka, K. P. Budohoski, *et al.*, ""optimal cerebral perfusion pressure" in poor grade patients after subarachnoid hemorrhage," *Neurocritical care*, vol. 13, no. 1, pp. 17–23, 2010.

[25] M. Czosnyka, Z. Czosnyka, and P. Smielewski, "Pressure reactivity index: Journey through the past 20 years," *Acta Neurochirurgica*, vol. 159, no. 11, pp. 2063–2065, 2017.

[26] C. Zweifel, G. Castellani, M. Czosnyka, *et al.*, "Non-invasive monitoring of cerebrovascular reactivity with near infrared spectroscopy in head-injured patients," *Journal of neurotrauma*, vol. 27, no. 11, pp. 1951–1958, 2010.

[27] T. Svedung Wettervik, T. Howells, P. Enblad, and A. Lewén, "Temporal neurophysiological dynamics in traumatic brain injury: Role of pressure reactivity and optimal cerebral perfusion pressure for predicting outcome," *Journal of neurotrauma*, vol. 36, no. 11, pp. 1818–1827, 2019.

[28] M. Rozanek, J. Skola, L. Horakova, and V. Trukhan, "Effect of artifacts upon the pressure reactivity index," *Scientific Reports*, vol. 12, no. 1, pp. 1–8, 2022.

[29] C. Dias, M. J. Silva, E. Pereira, *et al.*, "Optimal cerebral perfusion pressure management at bedside: A single-center pilot study," *Neurocritical care*, vol. 23, no. 1, pp. 92–102, 2015.

[30] B. Depreitere, F. Güiza, G. Van den Berghe, *et al.*, "Pressure autoregulation monitoring and cerebral perfusion pressure target recommendation in patients with severe traumatic brain injury based on minute-by-minute monitoring data," *Journal of neurosurgery*, vol. 120, no. 6, pp. 1451–1457, 2014.

[31] M. Czosnyka, P. Smielewski, P. Kirkpatrick, S. Piechnik, R. Laing, and J. Pickard, "Continuous monitoring of cerebrovascular pressure-reactivity in head injury," in *Intracranial Pressure and Neuromonitoring in Brain Injury*, Springer, 1998, pp. 74–77.

[32] M. J. Aries, M. Czosnyka, K. P. Budohoski, *et al.*, "Continuous determination of optimal cerebral perfusion pressure in traumatic brain injury," *Critical care medicine*, vol. 40, no. 8, pp. 2456–2463, 2012.

[33] M. Jaeger, M. U. Schuhmann, M. Soehle, and J. Meixensberger, "Continuous assessment of cerebrovascular autoregulation after traumatic brain injury using brain tissue oxygen pressure reactivity," *Critical care medicine*, vol. 34, no. 6, pp. 1783–1788, 2006.

[34] T. Howells, U. Johnson, T. McKelvey, and P. Enblad, "An optimal frequency range for assessing the pressure reactivity index in patients with traumatic brain injury," *Journal of clinical monitoring and computing*, vol. 29, no. 1, pp. 97–105, 2015.

[35] M. Czosnyka, P. Hutchinson, M. Balestreri, M. Hiler, P. Smielewski, and J. Pickard, "Monitoring and interpretation of intracranial pressure after head injury," in *Brain Edema XIII*, Springer, 2006, pp. 114–118.

[36] D. K. Radolovich, M. Czosnyka, I. Timofeev, *et al.*, "Reactivity of brain tissue oxygen to change in cerebral perfusion pressure in head injured patients," *Neurocritical care*, vol. 10, no. 3, pp. 274–279, 2009.

[37] J. K. Yue, M. J. Vassar, H. F. Lingsma, *et al.*, "Transforming research and clinical knowledge in traumatic brain injury pilot: Multicenter implementation of the common data elements for traumatic brain injury," *Journal of neurotrauma*, vol. 30, no. 22, pp. 1831–1844, 2013.

[38] C. O. Tan, "Defining the characteristic relationship between arterial pressure and cerebral flow," *Journal of applied physiology*, vol. 113, no. 8, pp. 1194–1200, 2012.

[39] R. Zhang, J. H. Zuckerman, C. A. Giller, and B. D. Levine, "Transfer function analysis of dynamic cerebral autoregulation in humans," *American Journal of Physiology-Heart and Circulatory Physiology*, vol. 274, no. 1, H233–H241, 1998.

[40] T. Lescot, L. Naccache, M. Bonnet, L. Abdennour, P. Coriat, and L. Puybasset, "The relationship of intracranial pressure lundberg waves to electroencephalograph fluctuations in patients with severe head trauma," *Acta neurochirurgica*, vol. 147, no. 2, pp. 125–129, 2005.

[41] J. Hamner, M. A. Cohen, S. Mukai, L. A. Lipsitz, and J. A. Taylor, "Spectral indices of human cerebral blood flow control: Responses to augmented blood pressure oscillations," *The Journal of physiology*, vol. 559, no. 3, pp. 965–973, 2004.

[42] R. Steinmeier, C. Bauhuf, U. Hübner, *et al.*, "Slow rhythmic oscillations of blood pressure, intracranial pressure, microcirculation, and cerebral oxygenation: Dynamic interrelation and time course in humans," *Stroke*, vol. 27, no. 12, pp. 2236–2243, 1996.

[43] E. Sorrentino, J. Diedler, M. Kasprowicz, *et al.*, "Critical thresholds for cerebrovascular reactivity after traumatic brain injury," *Neurocritical care*, vol. 16, pp. 258–266, 2012.

[44] L. Rivera-Lara, A. Zorrilla-Vaca, R. Geocadin, *et al.*, "Predictors of outcome with cerebral autoregulation monitoring: A systematic review and meta-analysis," *Critical care medicine*, vol. 45, no. 4, pp. 695–704, 2017.

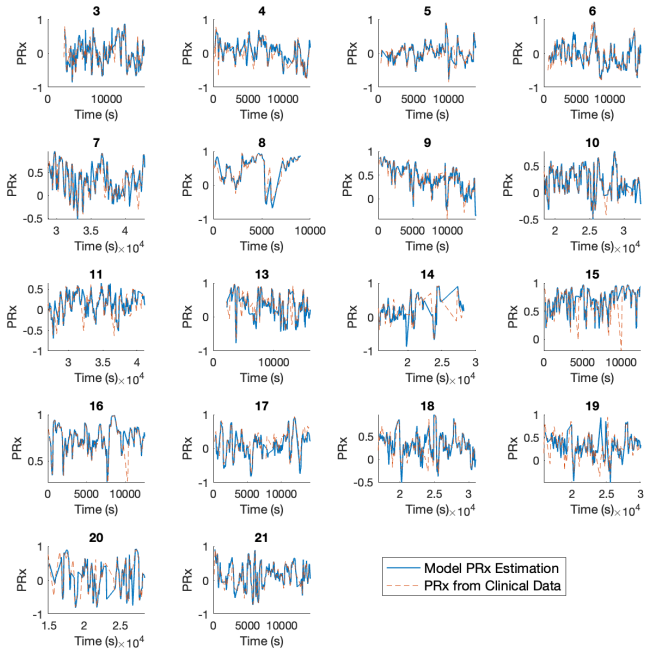

Fig. 1. Validation of PRx against clinical PRx datasets. Blue indicated our lagged PRx estimate. Red represents PRx estimate output by clinical PRx datasets

[45] F. A. Zeiler, J. Donnelly, L. Calviello, *et al.*, "Validation of pressure reactivity and pulse amplitude indices against the lower limit of autoregulation, part i: Experimental intracranial hypertension," *Journal of neurotrauma*, vol. 35, no. 23, pp. 2803–2811, 2018.

[46] F. A. Zeiler, J. K. Lee, P. Smielewski, M. Czosnyka, and K. Brady, "Validation of intracranial pressure-derived cerebrovascular reactivity indices against the lower limit of autoregulation, part ii: Experimental model of arterial hypotension," *Journal of neurotrauma*, vol. 35, no. 23, pp. 2812–2819, 2018.

[47] C. E. Shannon, "A mathematical theory of communication," *The Bell system technical journal*, vol. 27, no. 3, pp. 379–423, 1948.

[48] L. Riemann, E. Beqiri, P. Smielewski, *et al.*, "Low-resolution pressure reactivity index and its derived optimal cerebral perfusion pressure in adult traumatic brain injury: A center-tbi study," *Critical care*, vol. 24, no. 1, pp. 1–12, 2020.

VI. Supplemental Figures

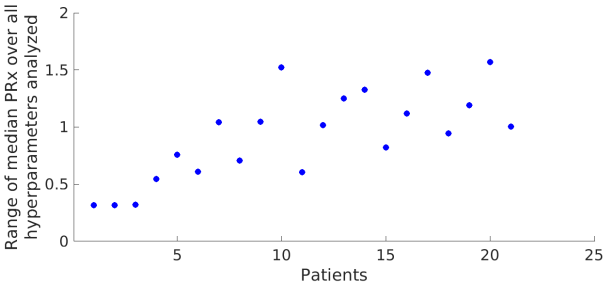

Fig. 2. Range of median PRx values over all hyperparameters analyzed